Computations on thin non-inhibited hyperbolic elastic shells. Benchmarks for membrane locking

Daniel CHOÏ *

January 19, 1999

Abstract

We study the bending limit problem of shells in relation with the membrane locking, encountered in finite element computation of non-inhibited very thin shells. Using a new approach of the theory of inextensional displacements (or infinitesimal bendings) we solve the bending limit problem in the case of a clamped hyperbolic paraboloid. We use then this solution to validate computations which can be used as bench-marks for the membrane locking. Such configuration, non-inhibited hyperbolic very thin shells, usually lacks in numerical 'validation'.

1 Introduction

An elastic shell is said to be *non-inhibited* if its middle surface admits *inextensional displacements* (or infinitesimal bendings), *i.e.* displacements leaving the metrics unchanged in the linearized sense. Otherwise, the shell is said inhibited (equivalently, its middle surface is said *geometrically rigid*) [18].

We emphasize on the fact that the inhibition property depends on the geometry and the boundary conditions and even the presence of edges (in the sense of folds [10]), but is totally independent of the considered material.

The natural trend of a thin elastic non-inhibited shell is to perform bendings, since such deformations are costless in energy than membrane deformation. This heuristic assertion is confirmed by the asymptotic analysis with thickness $\to 0$ of various linear models of shell (Koiter and Naghdi), even from 3D-elasticity [18, 19, 20, 6, 17].

The membrane locking phenomenon in computation of thin non-inhibited elastic shells is a serious deterioration of the finite element approximation as the thickness tends towards zero [8, 16]. A fine analysis showed that the membrane locking was due (at least in part) to a lacking of the computation to approximate properly the bending deformations [12, 7]. Thus, it is an exclusive phenomenon of the non-inhibited case of shells. Some numerical problems exist also for inhibited shells but they are from a different nature, we do not consider them here [15].

In a previous paper [12], it has been shown that membrane locking should always occurs for any finite element schemes pretending universality in computations of very thin shells, conformal or non conformal. In fact, our pessimistic point of view is to be nuanced, in its interpretation. Although, membrane locking should always occurs, it is not clear that such

*Laboratoire de Mécanique, Université de Caen Basse-Normandie, 14000 Caen and LMM, Université Pierre et Marie Curie, 75005 Paris, France – email: choi@lmm.jussieu.fr or choi@meca.unicaen.fr

locking is awkward: it may appear significant only for very small thickness possibly without physical interpretation. We can refer this as a kind of 'robustness' to the membrane locking. For instance, higher order finite element schemes such as Ganev-Argyris are accepted to be more 'robust' than lower order ones [7, 12].

We believe that since the membrane locking is unavoidable, effort should be directed in the ways to alleviate it, possibly using existing schemes.

Here, our intention is not to give an answer to the membrane locking robustness question. But in this objective, the bench-marks are essentials, see [12, 7]. We propose here bench-marks concerning non-inhibited hyperbolic shells. They are based on the resolution of the bending limit problem for non-inhibited shells when the thickness goes to zero. We shall consider two configurations (denoted as A and B) on the basis of clamped hyperbolic paraboloids, for which the set of inextensional displacement is completely determined. A first resolution of the bending limit problem was presented in [11] (referred as configuration A in the section 4 of this paper).

Actually, the bending limit solution will not be a bench-mark in itself. It is a validation test for the asymptotic behavior of a (non-inhibited) shell procedure as the thickness goes to zero. Using classical finite element scheme (Ganev-Argyris) to perform computations, we can validate them on the basis of the comparison with the solution of the bending limit problem. If the asymptotic behavior is consistent, the accuracy of the approximation is then shown. It is the case for the computations we make on two configurations of clamped non-inhibited hyperbolic paraboloid at the end of this paper. We propose then the results of these computations as bench-marks for the membrane locking. Up to our knowledge, such benchmark lacks in the literature.

This paper is organized as follow : after this introduction, in section 2, we recall briefly the asymptotic behavior of non-inhibited elastic shells as thickness goes to zero, and its consequences on the approximation. Section 3 deals with the bending limit problem. First, we expose our new approach of the theory of inextensional displacement. It is based on the notion of associated infinitesimal rotation field the partial derivatives of which constitute a space, denoted by $\boldsymbol{R}(S)$, isomorphic with the space of inextensional displacement denoted by$\boldsymbol{G}$. This will give the peculiar (extremely simple) expression of the linearized change of curvature tensor $\rho_{\alpha\beta}$ when the displacements are inextensional. This find an application in the expression of the bending energy bilinear form a_f, and then gives a new formulation of the bending limit problem. Section 4 is then devoted to the resolution of the bending limit problem (2.2) in the two considered cases. One case will be solved in a somehow analytical way. The other one will be approximated by Galerkin (finite element) projection. We end the section with a remark on the lack of smoothness of the solution of the bending limit problem. Last, in section 5, we compare with some numerical computations performed with the MODULEF code using Ganev-Argyris thin shell's finite element, leading to the bench-marks.

We end this introduction with some notations and conventions used in this paper.

$\mathcal{E}$ denotes the Euclidean space referred to an orthonormal frame $(O, \boldsymbol{e}_1, \boldsymbol{e}_2, \boldsymbol{e}_3)$. In this paper, we shall consider homogeneous and isotropic linearly elastic shell S_ϵ with constant thickness ϵ. They are defined with a middle surface S

$$S_\epsilon = S \times [-\frac{\epsilon}{2}, +\frac{\epsilon}{2}].$$

A surface S will be given by a map $(\Omega, \boldsymbol{r})$ where $\Omega \subset \mathbb{R}^2$ and $\boldsymbol{r}$ denotes the position vector. The parameters on Ω are x and y instead of the usual y^1 and y^2 for readability reasons.

The Latin (resp. Greek) indices or exponents belongs to the set $\{1,2,3\}$ (resp. $\{1,2\}$). The Einstein's summation convention will be used. The partial derivatives are denoted in indices with a preceding comma. The variables x and y are respectively associated with the numbers 1 and 2. For some vector field $\boldsymbol{u}$ defined on Ω we write

$$\boldsymbol{v}_{,1} = \frac{\partial \boldsymbol{v}}{\partial x} \qquad \boldsymbol{v}_{,2} = \frac{\partial \boldsymbol{v}}{\partial y}.$$

Of course the same rule holds for scalar functions.

In a classical way, we define the covariant basis on each point of S. It is constituted by the two *tangent* vectors

$$\boldsymbol{a}_\alpha = \boldsymbol{r}_{,\alpha}$$

and the unit normal vector $\boldsymbol{a}_3$; we define furthermore the coefficient

$$a = ||\boldsymbol{a}_1 \wedge \boldsymbol{a}_2||^2.$$

The contravariant basis is $(\boldsymbol{a}^1, \boldsymbol{a}^2, \boldsymbol{a}^3)$, defined by duality with the covariant basis, with the use of the Kronecker's symbol δ_i^j

$$\boldsymbol{a}_i.\boldsymbol{a}^j = \delta_i^j.$$

The coefficients of the first and second fundamental form are respectively

$$\begin{aligned} a_{\alpha\beta} &= \boldsymbol{a}_\alpha.\boldsymbol{a}_\beta \\ b_{\alpha\beta} &= \boldsymbol{a}_{\alpha,\beta}.\boldsymbol{a}_3. \end{aligned}$$

Let $\boldsymbol{u}$ be a displacement on S and let $\tilde{S}$ be the deformed surface, given by the map $(\Omega, \boldsymbol{r}+\boldsymbol{u})$. In this paper, we suppose that $\boldsymbol{u}$ is sufficiently small in order to stay in linearized framework with respect to the displacement.

The linearized tensor of deformation $\gamma_{\alpha\beta}(\boldsymbol{u})$ and the linearized tensor of curvature variation $\rho_{\alpha\beta}(\boldsymbol{u})$, see [4], are given by the following expressions

$$\begin{aligned} \gamma_{\alpha\beta}(\boldsymbol{u}) &= \frac{1}{2}(u_{\beta,\alpha} + u_{\alpha,\beta}) - \Gamma^\lambda_{\alpha\beta} u_\lambda - b_{\alpha\beta} u_3. \\ \rho_{\alpha\beta}(\boldsymbol{u}) &= u_{3,\alpha\beta} - \Gamma^\lambda_{\alpha\beta} u_{3,\lambda} + b^\lambda_\beta (u_{\lambda,\alpha} - \Gamma^\sigma_{\lambda\alpha} u_\sigma) + b^\lambda_\alpha (u_{\lambda,\beta} - \Gamma^\sigma_{\lambda\beta} u_\sigma), \\ &\quad + (b^\lambda_{\beta,\alpha} + \Gamma^\sigma_{\alpha\sigma} b^\lambda_\beta - \Gamma^\sigma_{\alpha\beta} b^\lambda_\alpha) u_\lambda - b_{\alpha\sigma} b^\sigma_\beta u_3, \end{aligned}$$

where $\Gamma^\lambda_{\alpha\beta} = \boldsymbol{a}^\lambda.\boldsymbol{a}_{\alpha,\beta}$ are the Christoffel's symbols and $b^\alpha_\beta = a^{\alpha\sigma} b_{\sigma\beta}$, with $a^{\alpha\beta} = \boldsymbol{a}^\alpha.\boldsymbol{a}^\beta$. We point out that these expressions will not be used in the sequel as we shall give alternate expressions in section 3.

Noting the space of kinematically admissible displacement by $\boldsymbol{V}$, we define the subspace of kinematically admissible inextensional displacement by

$$\boldsymbol{G} = \{\boldsymbol{u} \in \boldsymbol{V} / \gamma_{\alpha\beta}(\boldsymbol{u}) = 0\}$$

whereas the subset of inextensional displacement without kinematic boundary condition is denoted as

$$\tilde{\boldsymbol{G}} = \left\{\boldsymbol{u} \in \boldsymbol{H}^2(\Omega) / \gamma_{\alpha\beta}(\boldsymbol{u}) = 0\right\}.$$

In fact we have

$$\boldsymbol{G} = \tilde{\boldsymbol{G}} \cap \boldsymbol{V}.$$

2 The membrane locking phenomenon and non-inhibited shells

2.1 Asymptotic behavior of non-inhibited elastic shells, when the thickness tends to zero

Let us consider an homogeneous and isotropic linearly elastic shell S_ϵ with constant thickness ϵ and middle surface S. In the Koiter's framework, the asymptotic study shows that when the shell is non-inhibited (S is not geometrically rigid, i.e. $\boldsymbol{G} \neq \{0\}$), the solutions $\boldsymbol{u}^\epsilon$ of (2.1) converge (when the $\epsilon \longrightarrow 0$) to the solution of the bending problem (2.2). We have :

$$\boldsymbol{u}^\epsilon \longrightarrow \boldsymbol{u}^0 \in \boldsymbol{G}, \ \textit{strongly in } \boldsymbol{V}$$

where $\boldsymbol{u}^\epsilon$ is the solution of the mechanical problem with the Koiter's linear model :

$$\begin{cases} \text{Find a displacement } \boldsymbol{u}^\epsilon \in \boldsymbol{V} \text{ such that} \\ \epsilon a^m(\boldsymbol{u}^\epsilon, \boldsymbol{v}) + \epsilon^3 a^f(\boldsymbol{u}^\epsilon, \boldsymbol{v}) = \langle \boldsymbol{f}^\epsilon, \boldsymbol{v} \rangle \ \forall \boldsymbol{v} \in \boldsymbol{V}, \end{cases} \tag{2.1}$$

and $\boldsymbol{u}^0$ is the solution of the bending limit problem

$$\begin{cases} \text{Find a displacement } \boldsymbol{u}^0 \in \boldsymbol{G} \text{ such that} \\ a^f(\boldsymbol{u}^0, \boldsymbol{v}) = \langle \boldsymbol{f}, \boldsymbol{v} \rangle \ \forall \boldsymbol{v} \in \boldsymbol{G}, \end{cases} \tag{2.2}$$

with

$$\boldsymbol{f}^\epsilon = \epsilon^3 \boldsymbol{f}, \tag{2.3}$$

$\boldsymbol{f}$ independent of ϵ and for homogeneous and isotropic elastic shells, the energy bilinear forms of bending and membrane deformation are

$$a^f(\boldsymbol{u}, \boldsymbol{v}) = \frac{1}{12} \int_\Omega A^{\alpha\beta\lambda\mu} \rho_{\alpha\beta}(\boldsymbol{u}) \rho_{\lambda\mu}(\boldsymbol{v}) dS$$
$$a^m(\boldsymbol{u}, \boldsymbol{v}) = \int_\Omega A^{\alpha\beta\lambda\mu} \gamma_{\alpha\beta}(\boldsymbol{u}) \gamma_{\lambda\mu}(\boldsymbol{v}) dS$$

with the elasticity coefficients

$$A^{\alpha\beta\lambda\mu} = \frac{E}{2(1+\nu)} \left[a^{\alpha\lambda} a^{\beta\mu} + a^{\alpha\mu} a^{\beta\lambda} + \frac{2\nu}{1-\nu} a^{\alpha\beta} a^{\lambda\mu} \right],$$

where E is Young module and ν is the Poisson coefficient.

With $\boldsymbol{V} = \{\boldsymbol{u} \in H^1 \times H^1 \times H^2 + \textit{kinematical boundary conditions}\}$ the variational problem (2.1) stands in Lax-Milgram framework and hence, has a unique solution, see [4].

In the sequel, we shall refer to the problem (2.1) with external forces (2.3) as the Koiter's [linear] problem. Problem (2.2) will be referred as the bending limit problem.

Note that in the case where $\boldsymbol{G} = \{0\}$, the solutions $\boldsymbol{u}^\epsilon$ of the Koiter's problem converge to zero, see [20].

Remark 1. In this paper we consider Koiter's linear model, but analogous discussion and conclusion hold true for Naghi's model.

2.2 Non-robustness of FEM for thin elastic shells and Membrane locking

In [12], the incompatibility of the inextensional displacements with the polynomial has been shown. It implies the same incompatibility with all polynomial finite element's discretized space. This leads to the locking phenomenon. Let us recall that briefly.

We note by $\boldsymbol{V}_h$ a set of (discrete) spaces such that $\forall \boldsymbol{u} \in \boldsymbol{V}$, there exists a $\boldsymbol{v}_h \in \boldsymbol{V}_h$ such that $\boldsymbol{v}_h \longrightarrow \boldsymbol{v}$ in $\boldsymbol{V}$ when the parameter $h \longrightarrow 0$. The cases where $\boldsymbol{V}_h \not\subset \boldsymbol{V}$ (non conformal methods) are included.

If we denote by $\boldsymbol{u}_h^\epsilon$ the Galerkin approximation in $\boldsymbol{V}_h$ of $\boldsymbol{u}^\epsilon$, the solution of koiter's problem (2.1), the asymptotic behavior of $\boldsymbol{u}_h^\epsilon$ when $\epsilon \to 0$, is similar to that of $\boldsymbol{u}^\epsilon$:

$$\boldsymbol{u}_h^\epsilon \longrightarrow \boldsymbol{u}_h^0 \in \boldsymbol{V}.$$

where $\boldsymbol{u}_h^0$ belong to the set $\boldsymbol{G}_h = \boldsymbol{G} \cap \boldsymbol{V}_h$, and is the solution of the approximated bending limit problem

$$\begin{cases} \text{Find } \boldsymbol{u}_h^0 \in \boldsymbol{G}_h = \boldsymbol{G} \cap \boldsymbol{V}_h \\ a^f(\boldsymbol{u}_h^0, \boldsymbol{v}) = \langle \boldsymbol{f}, \boldsymbol{v} \rangle \quad \forall \boldsymbol{v} \in \boldsymbol{G}_h \end{cases}$$

We have the following diagram :

$$\begin{array}{ccc} \boldsymbol{u}_h^\epsilon \in \boldsymbol{V}_h & \xrightarrow{h \to 0} & \boldsymbol{u}^\epsilon \in \boldsymbol{V} \\ \Big\downarrow \epsilon \to 0 & & \Big\downarrow \epsilon \to 0 \\ \boldsymbol{u}_h^0 \in \boldsymbol{G}_h & & \boldsymbol{u}^0 \in \boldsymbol{G} \end{array} \tag{2.4}$$

If the diagram is commutative, the scheme is said *robust* in the sense of Babuska and Suri [2], then the approximation is membrane locking free. Unfortunately, this is not the case since $\boldsymbol{G}_h$ is always reduced to $\{0\}$ for some surfaces (most of the surfaces in fact), see[12] for some examples, including the case of the hyperbolic paraboloid.

Actually in [12], the incompatibility $\boldsymbol{G}_h = \{0\}$ is shown by proving $\tilde{\boldsymbol{G}} \cap \mathbb{P}_n(\mathbb{R}^2) = \{0\}$, where $\mathbb{P}_n(\mathbb{R}^2)$ is the set of polynomial displacements of order n, for any n. In other words, the incompatibility and thus the non-robustness is shown without considering the kinematic boundary conditions. Nethertheless, the boundary conditions can also be involved to prove $\boldsymbol{G}_h = \{0\}$ by a kind of propagation element by element in the case of hyperbolic shell, as in [6], similar to that of [1]. In fact the causes of incompatibility are obviously multiple.

Anyway, although such identification should be useful, possibly giving indication to alleviate the locking such as using a mesh topology taking in account some special geometric properties (asymptotic lines) of the shell, see [7], the incompatibility shown in [12] are rhedibitory since it is independent of the boundary conditions, the mesh topology or the order of polynomials involved, even for non-conformal schemes such as widely used DKT (Discrete Kirchoff Triangle).

This somehow pessimistic assertion underline the importance of bench-mark. It seems that until recently, the inhibited or non-inhibited character was not taken in account, although it plays an essential role in the membrane locking phenomenon, see [12] and [7]. Up to our knowledge a bench-mark concerning a non-inhibited hyperbolic shells lacks.

2.3 Benchmarks for membrane locking

On the basis of the diagram (2.4), we consider the limit bending problem and a set of $\boldsymbol{u}_h^\epsilon \subset \boldsymbol{V}_h$, solution of Koiter's approximated problem with (2.3), for decreasing values of the mesh step h and of the thickness ϵ.

By fixing the thickness ϵ, the value $\boldsymbol{u}_h^\epsilon$ converge as $h \to 0$. From this convergence we may extrapolate a limit value $\boldsymbol{u}_0^\epsilon$, or at least take the value given by the finest mesh. According to diagram (2.4), the "extrapolated" solutions $\boldsymbol{u}_0^\epsilon$ should converge to the bending limit solution, even if the convergence might appears "slow" with respect to the thickness. If it is the case, the accuracy of the results obtained is showed and can be considered as a valid benchmark.

On another hand by fixing h and making $\epsilon \to 0$, one will find the numerical solution go away from the solution of the bending problem (in fact as in most cases the subspace $\boldsymbol{G}_h = \{0\}$, the results will go to zero). It is the membrane locking, even though this might appears for very small thicknesses.

From this point of view, the solution of the bending limit problem constitutes a validation test.

3 The bending limit problem for non-inhibited shells

In this section, we study the limit problem of non-inhibited shells, when the thickness ϵ converge to zero (for external applied forces $\boldsymbol{f}^\epsilon = \epsilon^3 \boldsymbol{f}$). As we recalled in the preceding section, it is a problem lying in the subset $\boldsymbol{G}$ of inextensional displacements (or bendings). Using a new approach of this theory, we give a new formulation of the limit bending problem. This new formulation will be the key to our resolution, explicit for a case of hyperbolic paraboloid clamped along a generator.

3.1 A rotation approach of the inextensional displacement theory. The derived bending system.

We describe here a rotation approach of the inextensional displacement theory. It has been introduced in [9] to obtain rigidity theorems on edges. We refer to [10] for a throughout description on this topic.

Let $\boldsymbol{u}$ be a displacement on a surface S given by a map $(\Omega, \boldsymbol{r})$. We recall that $\boldsymbol{u}$ is said inextensional if it leaves the intrinsic metrics unchanged, that is to say if $\gamma_{\alpha\beta}(\boldsymbol{u}) = 0$. More precisely, is $\tilde{a}_{\alpha\beta}$ denote the coefficients of the first fundamental form of the deformed surface, we have

$$2\gamma_{\alpha\beta}(\boldsymbol{u}) = \tilde{a}_{\alpha\beta} - a_{\alpha\beta} = (\boldsymbol{a}_\alpha + \boldsymbol{u}_{,\alpha}).(\boldsymbol{a}_\beta + \boldsymbol{u}_{,\beta}) - a_{\alpha\beta}.$$

So that, by linearization, any inextensional displacement $\boldsymbol{u}$ must satisfy the bending system

$$\boldsymbol{a}_\alpha.\boldsymbol{u}_{,\beta} + \boldsymbol{a}_\beta.\boldsymbol{u}_{,\alpha} = 0 \tag{3.1}$$

Classically, see [23], there is a unique vector field $\boldsymbol{\omega}$, called associated infinitesimal rotation field satisfying the relations :

$$\begin{aligned} \boldsymbol{u}_{,1} &= \boldsymbol{\omega} \wedge \boldsymbol{a}_1 \\ \boldsymbol{u}_{,2} &= \boldsymbol{\omega} \wedge \boldsymbol{a}_2 \end{aligned} \tag{3.2}$$

One can see that rigid displacements are trivial solutions of the bending system (3.1) and the associated rotation fields are the constant vectors.

Writing the Schwarz equality (compatibility equality) $\boldsymbol{u}_{,12} = \boldsymbol{u}_{,21}$, we see that $\boldsymbol{\omega}$ necessarily satisfies the relation

$$\boldsymbol{\omega}_{,1} \wedge \boldsymbol{a}_2 = \boldsymbol{\omega}_{,2} \wedge \boldsymbol{a}_1. \tag{3.3}$$

Conversely, we have :

Proposition 3.1. *Any vector field $\boldsymbol{\omega}$ satisfying (3.3) determine a unique inextensional displacement $\boldsymbol{u}$ (modulo a rigid displacement). By quadrature, we have explicitly :*

$$\begin{aligned} \boldsymbol{u}(x,y) = &\int_0^{y^1} \boldsymbol{\omega}_{,1}(t,y) \wedge [\boldsymbol{r}(x,y) - \boldsymbol{r}(t,y)]dt \\ &+ \int_0^{y^2} \boldsymbol{\omega}_{,2}(0,s) \wedge [\boldsymbol{r}(x,y) - \boldsymbol{r}(0,s)]ds. \end{aligned} \tag{3.4}$$

Let us introduce the notation $\boldsymbol{w}_\alpha$ for the partial derivatives of a rotation field $\boldsymbol{\omega}$:

$$\boldsymbol{w}_\alpha = \boldsymbol{\omega}_{,\alpha}.$$

Taking the scalar product of (3.3) with $\boldsymbol{a}_\alpha$, we have

$$\boldsymbol{w}_\alpha.\boldsymbol{a}_3 = 0.$$

So that

Proposition 3.2. *The partial derivatives of a rotation field on a surface S are tangent to S.*

Let us express the fields $\boldsymbol{w}_\alpha$ by their contravariant components :

$$\boldsymbol{w}_\alpha = w_\alpha^1 \boldsymbol{a}_1 + w_\alpha^2 \boldsymbol{a}_2.$$

As the $\boldsymbol{w}_\alpha$ must satisfy the compatibility equality $\boldsymbol{w}_{1,2} = \boldsymbol{w}_{2,1}$, the components w_α^β satisfy a first order partial differential equation system, see [10] :

$$w_{1,2}^1 + \Gamma_{2\lambda}^1 w_1^\lambda = w_{2,1}^1 + \Gamma_{1\lambda}^1 w_2^\lambda \tag{3.5a}$$

$$w_{1,2}^2 + \Gamma_{2\lambda}^2 w_1^\lambda = w_{2,1}^2 + \Gamma_{1\lambda}^2 w_2^\lambda \tag{3.5b}$$

$$b_{12} w_1^1 + b_{22} w_1^2 = b_{11} w_2^1 + b_{12} w_2^2 \tag{3.5c}$$

moreover, from (3.3), we obtain

$$w_1^1 + w_2^2 = 0. \tag{3.5d}$$

The system (3.5) is called derived bending system.

Proposition 3.3. *The subset $\tilde{\boldsymbol{G}} = \{\boldsymbol{u} \in \boldsymbol{H}^2 / \gamma_{\alpha\beta}(\boldsymbol{u} = 0\}$ of inextensional displacements on the surface S is isomorphic to the space*

$$\tilde{\boldsymbol{R}}(S) = \left\{ \begin{array}{c} (\boldsymbol{w}_1, \boldsymbol{w}_2) \in \boldsymbol{L}^2 \times \boldsymbol{L}^2 / \text{ the contravariant components of} \\ \boldsymbol{w}_1 \text{ and } \boldsymbol{w}_2 \text{ satisfy the derived bending system } (3.5) \end{array} \right\}$$

We denote the bijection between $\tilde{\boldsymbol{R}}(S)$ and $\tilde{\boldsymbol{G}}$, for any $\boldsymbol{u} \in \tilde{\boldsymbol{G}}$, by

$$R(\boldsymbol{u}) = (\boldsymbol{w}_1, \boldsymbol{w}_2) \in \tilde{\boldsymbol{R}}(S).$$

or abusively (but without ambiguity)

$$R(\boldsymbol{u}) = (w_\alpha^\beta).$$

We define also the corresponding isomorphic space of kinematically admissible inextensional displacements

$$\boldsymbol{R}(S) = R(\boldsymbol{G}).$$

Remark 2. The bending system (3.1) (hence, the derived bending system) is equivalent, in a sense to be precized, to a partial differential equations system of total order 2, the characteristic lines of which coincide with the asymptotic lines of the considered surface S. In other words, if S is an hyperbolic (resp. elliptic) surface then the nature of the bending system will be hyperbolic (resp. elliptic). The same rule stands for the derived bending system [10, 17].

3.2 Expression of the linearized change of curvature tensor $\rho_{\alpha\beta}$ for an inextensional displacement

In this subsection, we present the very simple expression the tensor $\rho_{\alpha\beta}(\boldsymbol{u})$ takes when $\boldsymbol{u}$ is an inextensional displacement. It is a result first announced in [11]. This is the key to our alternative formulation of the bending limit problem.

Proposition 3.4. *Let $\boldsymbol{u}$ be an inextensional displacement on the considered surface S and let $\rho_{\alpha\beta}(\boldsymbol{u})$ be the tensor of curvature variation. If we denote by w_α^λ the contravariant components of $(\boldsymbol{w}_1, \boldsymbol{w}_2) = R(\boldsymbol{u})$, the partial derivatives of the associated rotation field $\boldsymbol{\omega}$, we have :*

$$\left\{\begin{array}{lcl} \rho_{11}(\boldsymbol{u}) & = & -w_1^2\sqrt{a} \\ \rho_{22}(\boldsymbol{u}) & = & +w_2^1\sqrt{a} \\ \rho_{12}(\boldsymbol{u}) & = & \frac{1}{2}(w_1^1 - w_2^2)\sqrt{a}. \end{array}\right. \tag{3.6}$$

Proof. By definition the change of curvature tensor $\rho_{\alpha\beta}$ is the linearized difference between $\tilde{b}_{\alpha\beta}$ and $b_{\alpha\beta}$, where $\tilde{b}_{\alpha\beta}$ are the second fundamental form coefficients of the deformed surface.

$$\begin{aligned} \tilde{b}_{\alpha\beta} &= \tilde{\boldsymbol{a}}_3.\tilde{\boldsymbol{a}}_{\alpha,\beta} \\ &= (\boldsymbol{a}_3 + \boldsymbol{\omega}\wedge\boldsymbol{a}_3).(\boldsymbol{a}_{\alpha,\beta} + \boldsymbol{u}_{,\alpha\beta}) \\ &= (\boldsymbol{a}_3 + \boldsymbol{\omega}\wedge\boldsymbol{a}_3).(\boldsymbol{a}_{\alpha,\beta} + (\boldsymbol{\omega}\wedge\boldsymbol{a}_\alpha)_{,\beta}) \\ &= \boldsymbol{a}_3.\boldsymbol{a}_{\alpha,\beta} + (\boldsymbol{\omega}\wedge\boldsymbol{a}_3).\boldsymbol{a}_{\alpha,\beta} + \boldsymbol{a}_3.(\boldsymbol{\omega}\wedge\boldsymbol{a}_\alpha)_{,\beta} + (\boldsymbol{\omega}\wedge\boldsymbol{a}_3).(\boldsymbol{\omega}\wedge\boldsymbol{a}_\alpha)_{,\beta} \\ &= b_{\alpha\beta} + (\boldsymbol{\omega}\wedge\boldsymbol{a}_3).\boldsymbol{a}_{\alpha,\beta} + \boldsymbol{a}_3.(\boldsymbol{\omega}\wedge\boldsymbol{a}_{\alpha,\beta}) + \boldsymbol{a}_3.(\boldsymbol{w}_\beta\wedge\boldsymbol{a}_\alpha) + (\boldsymbol{\omega}\wedge\boldsymbol{a}_3).(\boldsymbol{\omega}\wedge\boldsymbol{a}_\alpha)_{,\beta} \\ &= b_{\alpha\beta} + \boldsymbol{a}_3.(\boldsymbol{w}_\beta\wedge\boldsymbol{a}_\alpha) + (\boldsymbol{\omega}\wedge\boldsymbol{a}_3).(\boldsymbol{\omega}\wedge\boldsymbol{a}_\alpha)_{,\beta}. \end{aligned}$$

Then, the linearized variation $\rho_{\alpha\beta}$ of the coefficients of the second fundamental form is

$$\rho_{\alpha\beta}(\boldsymbol{u}) = \boldsymbol{a}_3.(\boldsymbol{w}_\beta\wedge\boldsymbol{a}_\alpha) = \boldsymbol{a}_3.[(w_\alpha^\lambda\boldsymbol{a}_\lambda)\wedge\boldsymbol{a}_\alpha]. \tag{3.7}$$

Then, developing the last equality gives the expressions (3.6) □

3.3 Alternative formulation of the bending limit problem

With the new expressions of the change of curvature tensor $\rho_{\alpha\beta}$, we are able to give an alternate expression of the bending limit problem. Our main idea is to move the problem from the set of inextensional displacements $\boldsymbol{G}$ to the set of partial derivatives of rotation fields $\boldsymbol{R}(S)$.

The bending limit problem (2.2) is rewritten as

$$\left\{\begin{array}{l} \text{Find } w_\alpha^\lambda \in \boldsymbol{R}(S) \text{ such that} \\ \displaystyle\iint_\Omega A^{\alpha\beta\lambda\mu}c_{\alpha\nu}w_\beta^\nu c_{\lambda\sigma}\tilde{w}_\mu^\sigma\sqrt{a}dxdy = \langle\boldsymbol{f},\tilde{\boldsymbol{u}}\rangle \quad \forall\tilde{w}_\mu^\sigma \in \boldsymbol{R}(S) \end{array}\right. \tag{3.8}$$

where $(w_\alpha^\beta) = R(\boldsymbol{u})$ and $(\tilde{w}_\alpha^\beta) = R(\tilde{\boldsymbol{u}})$ and with

$$(c_{\alpha\beta}) = \sqrt{a}\begin{pmatrix} 0 & 1 \\ -1 & 0 \end{pmatrix}. \tag{3.9}$$

One can notice that $c_{\alpha\beta}$ defines an anti-symmetric covariant tensor of rank 2.

Apparently, the alternate formulation (3.8) is not less complex than the original one (2.2), the difficulties being moved from the space $\boldsymbol{G}$ to the space $\boldsymbol{R}(S)$, and there is still a differential system to be satisfied. In fact, the wining move is in the new expression of the change of curvature tensor $\rho_{\alpha\beta}$, as it contains no derivatives on the new unknowns (w_α^β).

4 Resolution of the bending limit problem

In this section, we solve the bending limit problem, using the formulation (3.8), in special cases where the middle surface is a hyperbolic paraboloid. The reason of this choice is mainly that it is an hyperbolic surface example for which we are able to solve the bending limit problem.

We study two configurations of hyperbolic paraboloid with different kinematic boundary conditions. The surface is clamped along an asymptotic line in the first case (configuration A) and clamped along a boundary transverse the asymptotic lines in the second case (configuration B), giving respectively a totally non-inhibited shell and a partially inhibited shell. It illustrates the essential role played by asymptotic lines in the membrane locking problem, see [10, 12, 7].

Let S, all along the rest of this paper, be a hyperbolic paraboloid. We define S with the mapping $(\Omega, \boldsymbol{r})$:

$$\boldsymbol{r}(x,y) = x\boldsymbol{e}_1 + y\boldsymbol{e}_2 + cxy\boldsymbol{e}_3,$$

where Ω is a domain of $\mathbb{R}^2$ and c is given real constant. We can vary the geometry by taking different values of c. For instance with small values of c, the corresponding shell is shallow (not recommended as a test for the membrane locking).

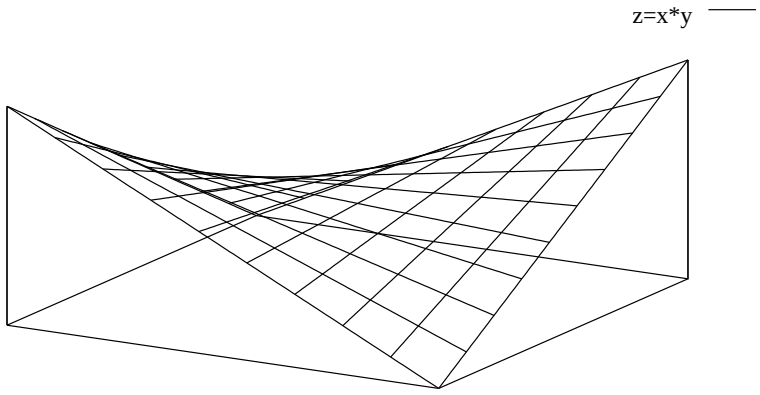

Figure 1: A hyperbolic paraboloid

S is a hyperbolic surface with the particularity to be double ruled, thus the asymptotic lines are the generators, see [22]. With this mapping, the expressions of various geometrical coefficients are

$$\boldsymbol{a}_1 = (1, 0, cy) \qquad \boldsymbol{a}^1 = \frac{1}{a}\left(1 + (cx)^2, -cxcy, cy\right)$$

$$\boldsymbol{a}_2 = (0, 1, cx) \qquad \boldsymbol{a}_2 = \frac{1}{a}\left(-cxcy, 1 + (cy)^2, cx\right)$$

$$\boldsymbol{a}_3 = \frac{1}{\sqrt{a}}(-cy, -cx, 1) \qquad \boldsymbol{a}^3 = \frac{1}{\sqrt{a}}(-cy, -cx, 1)$$

$$a = 1 + (cx)^2 + (cy)^2$$

$$
\begin{array}{lll}
a_{11} = 1 + (cy)^2, & a_{12} = cxcy, & a_{22} = 1 + (cx)^2 \\
a^{11} = \dfrac{1}{a}\left(1 + (cx)^2\right) & a^{12} = \dfrac{1}{a}(cxcy) & a^{22} = \dfrac{1}{a}\left(1 + (cy)^2\right) \\
b_{11} = 0 & b_{12} = \dfrac{c}{\sqrt{a}} & b_{22} = 0 \\
\Gamma^1_{12} = \dfrac{1}{a}(c^2 y) & \Gamma^2_{12} = \dfrac{1}{a}(c^2 x) & \Gamma^\beta_{\alpha\alpha} = 0.
\end{array}
$$

and the elasticity coefficients for homogeneous and isotropic elastic shells are

$$
\begin{aligned}
A^{1111} &= \frac{E}{12(1-\nu^2)} \frac{\left(1 + (cx)^2\right)^2}{a^2} \\
A^{1122} &= \frac{E}{12(1-\nu^2)} \frac{\left((cx)^2 (cy)^2 + \nu a\right)}{a^2} \\
A^{2222} &= \frac{E}{12(1-\nu^2)} \frac{\left(1 + (cy)^2\right)^2}{a^2}.
\end{aligned}
$$

We do not write the coefficients A^{1112}, A^{1212} or A^{1222} as we shall not use them in the sequel.

4.1 Inextensional displacements of a hyperbolic paraboloid

The description of inextensional displacement on hyperbolic paraboloid clamped along a generator (asymptotic line) is classical, see [13]. We shall recall it in the framework of the rotational approach of inextensional displacement theory given in subsection 3.1.

Let $\boldsymbol{u}$ be an inextensional displacement on S, let $\boldsymbol{\omega}$ be its associated rotation field and let $w^\lambda_\beta = R(\boldsymbol{u})$ be the contravariant components of the partial derivatives of $\boldsymbol{\omega}$. According to subsection 3.1 the coefficients w^λ_β satisfy the derived bending system (3.5) which becomes in this special case

$$
\left\{
\begin{array}{rcl}
w^1_{1,2} & = & w^1_{2,1} \\
w^2_{1,2} & = & w^2_{2,2} \\
w^1_1 & = & w^2_2
\end{array}
\right. \tag{4.1}
$$

and with (3.5d) ($w^1_1 + w^2_2 = 0$), we obtain

$$
\left\{
\begin{array}{ll}
w^1_1 & = 0 \\
w^2_2 & = 0 \\
w^1_{2,1} & = 0 \\
w^2_{1,2} & = 0.
\end{array}
\right. \tag{4.2}
$$

Thus (if Ω is convex) $\tilde{\boldsymbol{R}}(S)$ (hence, the subspace $\tilde{\boldsymbol{G}}$ of inextensional displacement) appears isomorphic to a product of two scalar functions spaces of one variable $\mathbb{L}^2_y \times \mathbb{L}^2_x$. More precisely, for any inextensional displacement $\boldsymbol{u} \in \boldsymbol{H}^2$, there is a unique couple of functions $(\phi_{\boldsymbol{u}1}, \phi_{\boldsymbol{u}2}) \in \mathbb{L}^2_y \times \mathbb{L}^2_x$ such that the partial derivatives of the associated rotation field $\boldsymbol{\omega}$ are given by

$$
\left\{
\begin{array}{ll}
\boldsymbol{\omega}_{,1}(x,y) & = \phi_{\boldsymbol{u}2}(x)\boldsymbol{a}_2(x,y) \\
\boldsymbol{\omega}_{,2}(x,y) & = \phi_{\boldsymbol{u}1}(y)\boldsymbol{a}_1(x,y).
\end{array}
\right. \tag{4.3}
$$

Then, applying the proposition 3.1 we obtain, modulo a rigid displacement

$$\boldsymbol{u}(x,y) = \int_0^x \phi_{\boldsymbol{u}2}(t)(\boldsymbol{e}_2 + ct\boldsymbol{y}\boldsymbol{e}_3) \wedge [(x-t)\boldsymbol{e}_1 + cy(x-t)\boldsymbol{e}_3]\, dt + \int_0^y \phi_{\boldsymbol{u}1}(s)(\boldsymbol{e}_1 + cs\boldsymbol{e}_3) \wedge [x\boldsymbol{e}_1 + (y-s)\boldsymbol{e}_2 + cxy\boldsymbol{e}_3]\, ds.$$

It suffices then to develop the last expression to obtain :

Proposition 4.1. *$\tilde{\boldsymbol{R}}(S)$ is isomorphic to $\mathbb{L}^2_y \times \mathbb{L}^2_x$. For any inextensional displacement $\boldsymbol{u}$ on the hyperbolic paraboloid S, there is a unique couple $(\phi_{\boldsymbol{u}1}, \phi_{\boldsymbol{u}2}) \in \mathbb{L}^2_y \times \mathbb{L}^2_x$, such that modulo a rigid displacement, we have*

$$\begin{aligned}\boldsymbol{u}(x,y) =& [cy\Phi_{\boldsymbol{u}2}(x) - c\Psi_{\boldsymbol{u}1}(y)]\,\boldsymbol{e}_1 + [c\Psi_{\boldsymbol{u}2}(x) - cx\Phi_{\boldsymbol{u}1}(y)]\,\boldsymbol{e}_2 \\ &- [\Phi_{\boldsymbol{u}2}(x) - \Phi_{\boldsymbol{u}1}(y)]\,\boldsymbol{e}_3,\end{aligned} \tag{4.4}$$

where the functions $\Phi_{\boldsymbol{u}\alpha}$ and $\Psi_{\boldsymbol{u}\alpha}$ are defined with $\phi_{\boldsymbol{u}\alpha}$ by quadrature

$$\Phi_{\boldsymbol{u}\alpha}(x) = \int_0^x \phi_{\boldsymbol{u}\alpha}(z)(x-z)dz \tag{4.5}$$

$$\Psi_{\boldsymbol{u}\alpha}(x) = \int_0^x \phi_{\boldsymbol{u}\alpha}(z)z(x-z)dz. \tag{4.6}$$

4.2 Configuration A – A totally non-inhibited clamped hyperbolic paraboloid

We consider here the case where the hyperbolic paraboloid is defined on a rectangular domain $\Omega = [x_0, x_1] \times [y_0, y_1]$ and is clamped all along the generator at $x = x_0$, denoted as σ. The remaining boundary is supposed free of any constraints. In the sequel it will be referred as the configuration A.

With the proposition 4.1, it is easy to show that such clamped shell is totally non-inhibited, *i.e.* on any part of the shell there is an admissible inextensional displacement on S different of zero.

Let $\boldsymbol{u}$ be an admissible inextensional displacement on S and let

$$R(\boldsymbol{u}) = (\phi_{\boldsymbol{u}1}, \phi_{\boldsymbol{u}2}) \in \mathbb{L}^2_x \times \mathbb{L}^2_y$$

be its associated functions correspondingly to the proposition 4.1. The boundary condition on σ implies $\boldsymbol{u}(x_0, y) = 0$, then we have also

$$\boldsymbol{u}_{,2}(x_0, y) = 0.$$

Denoting as before the rotation field by $\boldsymbol{\omega}$, it follows from (3.2)

$$\boldsymbol{\omega}(x_0, y) \wedge \boldsymbol{a}_2 = 0,$$

which implies, since $\boldsymbol{a}_{2,2}$ is colinear to $\boldsymbol{a}_2$,

$$\boldsymbol{\omega}_{,2}(x_0, y) \wedge \boldsymbol{a}_2 = 0.$$

In other words, $w^1_2 \equiv \phi_{\boldsymbol{u}1}$ vanishes along σ. Thus, we obtain the general expression of admissible inextensional displacement on the hyperbolic paraboloid S clamped along the generator σ :

$$\boldsymbol{u}(x,y) = cy\Phi_{\boldsymbol{u}2}(x)\boldsymbol{e}_1 + c\Psi_{\boldsymbol{u}2}(x)\boldsymbol{e}_2 - \Phi_{\boldsymbol{u}2}(x)\boldsymbol{e}_3, \tag{4.7}$$

where $\Phi_{\boldsymbol{u}2}$ and $\Psi_{\boldsymbol{u}2}$ are defined as in (4.5)-(4.6). Note that (4.7) is exact (i.e. not modulo a rigid displacement).

Conversely, it is clear that for any function $\phi_{\boldsymbol{u}2} \in \mathbb{L}^2_x$, last formula determines a unique admissible inextensional displacement on the hyperbolic paraboloid clamped along the generator σ.

We have shown that the admissible inextensional displacement subspace $\boldsymbol{G}$ is isomorphic to the space $\mathbb{L}^2[x_0, x_1]$ and the alternate formulation of the bending limit problem (4.9) will appear equivalent, in a certain sense, to an ordinary differential equation.

Indeed, with the simplifications of the hyperbolic paraboloid case, $\rho_{\alpha\beta}$ reduces to

$$\begin{cases} \rho_{11}(\boldsymbol{u}) = -\sqrt{a}\phi_{\boldsymbol{u}2} \\ \rho_{12}(\boldsymbol{u}) = 0 \\ \rho_{22}(\boldsymbol{u}) = 0. \end{cases} \tag{4.8}$$

Let $\boldsymbol{f} \in \mathbb{L}^{\boldsymbol{2}}$ be the external applied force of the limit bending problem. We have then :

$$\begin{cases} \text{Find } \boldsymbol{u}^0 \in \boldsymbol{G} \text{ such that} \\ \iint_\Omega A^{1111}(x,y)\rho_{11}(\boldsymbol{u}^0)\rho_{11}(\boldsymbol{v})ads = \langle \boldsymbol{f}, \boldsymbol{v} \rangle \quad \forall \boldsymbol{v} \in \boldsymbol{G}. \end{cases} \tag{4.9}$$

Let us decompose $\boldsymbol{f}$ in its Cartesian components

$$\boldsymbol{f} = f_i \boldsymbol{e}_i.$$

For any inextensional displacement $\boldsymbol{v}$ on S and it s associated function $\phi_{\boldsymbol{v}2}(= (\phi_{\boldsymbol{v}2}, 0) = R(\boldsymbol{u})x$ we have, with the notation of (4.5) :

$$\langle \boldsymbol{f}, \boldsymbol{v} \rangle = (cyf_1 - f_3)\Phi_{\boldsymbol{v}2}(x) + cf_2\Psi_{\boldsymbol{v}2}(x).$$

The bending limit problem therefore becomes :

$$\begin{cases} \text{Find } \phi_{\boldsymbol{u}2} \in \mathbb{L}^2_x \text{ such that} \\ \int_\Omega A^{1111}\phi_{\boldsymbol{u}2}\phi_{\boldsymbol{v}2}ads = \int_\Omega [(cyf_1 - f_3)\Phi_{\boldsymbol{v}2} + cf_2\Psi_{\boldsymbol{v}2}]\sqrt{a}ds \quad \forall \phi_{\boldsymbol{v}2} \in \mathbb{L}^2_x. \end{cases} \tag{4.10}$$

Introducing some intermediate functions :

$$\alpha(x) = \int_{y_0}^{y_1} A^{1111}(x,y)a\sqrt{a}dy, \tag{4.11}$$

$$\begin{cases} F_1(x) = \int_{y_0}^{y_1} yf_1(x,y)\sqrt{a}dy \\ F_2(x) = \int_{y_0}^{y_1} f_2(x,y)\sqrt{a}dy \\ F_3(x) = \int_{y_0}^{y_1} f_3(x,y)\sqrt{a}dy, \end{cases} \tag{4.12}$$

An equivalent formulation of the bending limit problem (3.8) writes

$$\begin{cases} \text{Find } \phi_{\boldsymbol{u}2} \in \mathbb{L}^2_x(x_0, x_1) \text{ such that} \\ \int_{x_0}^{x_1} \alpha\phi_{\boldsymbol{u}2}\phi_{\boldsymbol{v}}dx = \int_{x_0}^{x_1} [(cF_1 - F_3)\Phi_{\boldsymbol{v}} + cF_2\Psi_{\boldsymbol{v}}]dx \quad \forall \phi_{\boldsymbol{v}} \in L^2_x(x_0, x_1). \end{cases} \tag{4.13}$$

Proposition 4.2. *The unique solution of* (4.13) *is*

$$\phi_{\boldsymbol{u}}(x) = \frac{1}{\alpha(x)} \int_{x_0}^{x} \left(cF_1(t) - F_3(t) + cxF_2(t)\right)(x-t)dt. \tag{4.14}$$

The solution of the bending limit problem (2.2) *is then obtain from the expressions* (4.7) *and* (4.5)-(4.6)

Proof. Although non-classical, (4.13) is nearly a variational formulation of an ordinary second order differential equation. Formally, integrating by parts, we have

$$\begin{aligned}\int_{x_0}^{x_1} \alpha(x)\phi_{\boldsymbol{u}2}\phi_{\boldsymbol{v}2}dx = &\left[\alpha\phi_{\boldsymbol{u}2}\frac{d}{dx}(\Phi_{\boldsymbol{v}2})\right]_{x_0}^{x_1} - \left[\frac{d}{dx}(\alpha\phi_{\boldsymbol{u}2})\Phi_{\boldsymbol{v}2}\right]_{x_0}^{x_1} \\ &+ \int_{x_0}^{x_1} \frac{d^2}{dx^2}(\alpha(x)\phi_{\boldsymbol{u}2})\Phi_{\boldsymbol{u}2}dx\end{aligned}$$

As a consequence, since $\Phi_{\boldsymbol{v}2}(x_0) = \frac{d}{dx}\Phi_{\boldsymbol{v}2}(x_0) = 0$, a solution to problem (4.15)

$$\begin{cases} \text{Find } (\alpha\phi_{\boldsymbol{u}2}) \in \left\{ g \in H^2[x_0,x_1] \quad / \quad g(x_1) = \dfrac{d}{dx}g(x_1) = 0 \right\} \text{ such that} \\ \displaystyle\int_{x_0}^{x_1} \frac{d^2}{dx^2}(\alpha\phi_{\boldsymbol{u}2})\Phi_{\boldsymbol{v}2}dx = \int_{x_0}^{x_1} \left[(cF_1 - F_3)\Phi_{\boldsymbol{v}2} + cF_2\Psi_{\boldsymbol{v}2}\right]dx \quad \forall \phi_{\boldsymbol{v}2} \in \mathbb{L}^2[x_0,x_1] \end{cases} \tag{4.15}$$

is a solution to problem (4.13).

We exhibit now the solution of problem (4.15). Let us define the function

$$[\alpha\phi_{\boldsymbol{u}2}](x) = (\alpha\phi_A) - (\alpha\phi_B) \tag{4.16}$$

where

$$\begin{aligned}[\alpha\phi_A](x) &= \int_{x_1}^{x} (cF_1 - F_3)(x-t)dt \\ [\alpha\phi_B](x) &= \int_{x_1}^{x} (cxF_2)(x-t)dt.\end{aligned} \tag{4.17}$$

In order to prove that (4.16) is the solution of (4.15), we note that

$$\begin{aligned}\frac{d^2}{dx^2}(\alpha\phi_A) &= cF_1 - F_3 \\ \frac{d^2}{dx^2}(\alpha\phi_B) &= cxF_2\end{aligned} \qquad \forall x \in [x_0,x_1].$$

Then, taking the product of $\alpha\phi_A$ and $\alpha\phi_B$ with $\Phi_{\boldsymbol{v}2}$ and integrating from x_0 to x_1, we have

$$\begin{aligned}\int_{x_0}^{x_1} \frac{d^2}{dx^2}(\alpha\phi_A)\Phi_{\boldsymbol{v}2}dx &= \int_{x_0}^{x_1} (cF_1 - F_3)\Phi_{\boldsymbol{v}2}dx \\ \int_{x_0}^{x_1} \frac{d^2}{dx^2}(\alpha\phi_B)\Phi_{\boldsymbol{v}2}dx &\int_{x_0}^{x_1} cxF_2\Phi_{\boldsymbol{v}2}dx\end{aligned}$$

As $\Psi_{\boldsymbol{v}2}(x) = x\Phi_{\boldsymbol{v}2}(x)$, (4.13) follows. □

Though our resolution is valid for any given $\boldsymbol{f}$, we give some numerical examples by considering the case of uniform normal applied external forces

$$\boldsymbol{f}^\epsilon = \epsilon^3 \boldsymbol{f} = \epsilon^3 f \boldsymbol{a}_3, \quad f \in \mathbb{R}$$

In Cartesian components we have :

$$f_1 = \frac{-cfy}{\sqrt{a}}, \quad f_2 = \frac{-cfx}{\sqrt{a}}, \quad f_3 = \frac{f}{\sqrt{a}}$$

In this case, the intermediate functions becomes

$$\begin{aligned}
F_1(x) &= \int_{y_0}^{y_1} -fcy^2 dy = -cf\frac{1}{3}(y_1 - y_0)(y_1^2 + y_0 y_1 + y_0^2) \\
F_2(x) &= \int_{y_0}^{y_1} -fcxdy = -cfx(y_1 - y_0) \\
F_3(x) &= \int_{y_0}^{y_1} f dy = f(y_1 - y_0) \\
\alpha(x) &= \int_{y_0}^{y_1} \frac{E[1 + (cx)^2]^2}{12(1-\nu^2)\sqrt{a}} dy,
\end{aligned}$$

The inextensional displacement $\boldsymbol{u}$ solution of the bending limit problem being constructed according to the expressions (4.7) and (4.5)-(4.6).

In this special case where f is uniform, we are able to determinate the *analytical* expression of the solution $\phi_{\boldsymbol{u}2}$ of the equivalent formulation (4.15) of the bending limit problem. With the help of a formal computation software (Maple or MuPAD) we obtain

$$\begin{aligned}
\alpha(x) &= \frac{Ey[1 + (cx)^2]^2}{12c(1-\nu^2)} \left[\ln\left(cy_1 + \sqrt{a(x, y_1)}\right) - \ln\left(cy_0 + \sqrt{a(x, y_0)}\right)\right] \\
\phi_{\boldsymbol{u}2}(x) &= \frac{f(x - x_1)^2(y_0 - y_1)}{6\alpha(x)} \left[(cy_1)^2 + cy_1 cy_0 + (cx)^2 + 2cxcx_1 + (cy_0)^2 + 3\right]
\end{aligned} \tag{4.18}$$

The solution of the corresponding bending limit problem can then be computed by a simple numerical integration of the expressions (4.7) and (4.5)-(4.6).

As an example, $E = 28500$, $\nu = 0.3$, $x_0 = -1$, $x_1 = 1$, $y_0 = -1$, $y_0 = 1$, and $f = 1$, we get for the normal component u_3 at the point (1,1) of the displacement solution of the bending limit problem (2.2) for several values of the geometric parameter c

$c = 0.1$	$c = 0.5$	$c = 1$	$c = 2$	$c = 3$	$c = 5$
7.5845e-04	6.3066e-04	5.239101e-04	7.4901e-04	1.4429e-03	4.4456e-03

Table 1: Values of the normal component u_3 at point (1,1) for different geometries.

4.3 Configuration B – A partially inhibited hyperbolic paraboloid

In this section we consider the hyperbolic paraboloid S defined as above, but with a domain Ω defined with the four summit A, B, C and D of coordinates

$$\begin{array}{ll} A : (-1, 0) & B : (0, -1) \\ C : (1, 0) & D : (0, 1) \end{array}$$

In this example, we impose the clamping along the boundary AB and we suppose the rest of the boundary, free of any kinematic constraint.This constitutes the configuration B.

As for the configuration A, we prove first that configuration B is non-inhibited.

Proposition 4.3. *Let $\boldsymbol{u}$ be an admissible inextensional displacement on the hyperbolic paraboloid S clamped along the boundary AB (configuration B) . According to proposition 4.1 there is a unique couple $(\phi_{\boldsymbol{u}2}, \phi_{\boldsymbol{u}1}) \in \mathbb{L}^2_x[-1,1] \times \mathbb{L}^2_y[-1,1]$ such that $\boldsymbol{u}$ can be given by*

$$\begin{aligned}\boldsymbol{u}(x,y) =& [cy\Phi_{\boldsymbol{u}2}(x) - c\Psi_{\boldsymbol{u}1}(y)]\,\boldsymbol{e}_1 + [c\Psi_{\boldsymbol{u}2}(x) - cx\Phi_{\boldsymbol{u}1}(y)]\,\boldsymbol{e}_2 \\ & - [\Phi_{\boldsymbol{u}2}(x) - \Phi_{\boldsymbol{u}1}(y)]\,\boldsymbol{e}_3\end{aligned} \tag{4.19}$$

where

$$\Phi_{\boldsymbol{u}\alpha}(z) = \int_0^z \phi_{\boldsymbol{u}\alpha}(t)(z-t)dt$$
$$\Psi_{\boldsymbol{u}\alpha}(z) = \int_0^z \phi_{\boldsymbol{u}\alpha}(t)t(z-t)dt$$

Then we have furthermore

$$\begin{aligned}\phi_{\boldsymbol{u}1}(y) &= 0 \quad \forall y \in [-1,0] \\ \phi_{\boldsymbol{u}2}(x) &= 0 \quad \forall x \in [-1,0].\end{aligned}$$

and conversely.

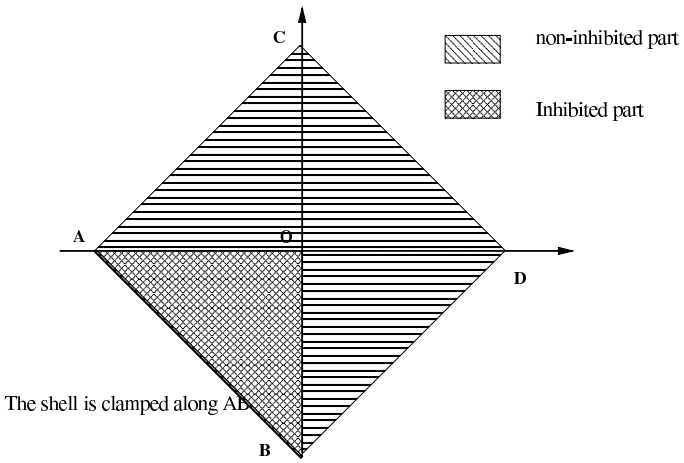

Figure 2: Configuration B

In other words, the hyperbolic paraboloid clamped along AB is partially inhibited in the triangle AOB, but admits inextensional displacements, non-trivial on the rest of the surface see fig 2. In fact, according to the definition, it is non-inhibited.

Proof. (of proposition 4.3). The clamping along the boundary AB can be considered as a Cauchy data for the bending system, and also for the derived bending system. As AB is transversal to the characteristic lines (generators), the classical uniqueness theorem for hyperbolic system shows that admissible inextensional displacements vanish necessarily in the dependence domain, *i.e.* in the triangle AOB.

According to proposition 3.1, it suffices then to verify that inextensional displacements defined as above vanish in AOB. □

In this framework, the limit problem (3.8) is

$$\begin{cases} \text{Find } (\phi_{\boldsymbol{u}2}, \phi_{\boldsymbol{u}1}) \in \mathbb{L}^2_x \times \mathbb{L}^2_y, \text{ such that } \forall \boldsymbol{v} \in \boldsymbol{G} \quad (\boldsymbol{v} = R^{-1}(\phi_{\boldsymbol{v}2}, \phi_{\boldsymbol{v}1})) \\ \int_\Omega [A^{1111}\phi_{\boldsymbol{u}2}\phi_{\boldsymbol{v}2} + A^{1122}\phi_{\boldsymbol{u}2}\phi_{\boldsymbol{v}1} + A^{2211}\phi_{\boldsymbol{u}1}\phi_{\boldsymbol{v}2} + A^{2222}\phi_{\boldsymbol{u}1}\phi_{\boldsymbol{v}1}] ads = \langle \boldsymbol{f}, \boldsymbol{v} \rangle, \end{cases}$$

Introducing the matrix $\mathbb{A}$:

$$\mathbb{A} = \begin{pmatrix} A^{1111} & -A^{1122} \\ -A^{1122} & A^{2222} \end{pmatrix},$$

it reads

$$\begin{cases} \text{Find } (\phi_{\boldsymbol{u}2}, \phi_{\boldsymbol{u}1}) \in \mathbb{L}^2_x \times \mathbb{L}^2_y, \text{ such that} \\ \int_\Omega \begin{pmatrix} \phi_{\boldsymbol{u}2} \\ \phi_{\boldsymbol{u}1} \end{pmatrix} \mathbb{A} \begin{pmatrix} \phi_{\boldsymbol{v}2} \\ \phi_{\boldsymbol{v}1} \end{pmatrix} ads = \langle \boldsymbol{f}, R^{-1}(\phi_{\boldsymbol{v}2}, \phi_{\boldsymbol{v}1}) \rangle \quad \forall (\phi_{\boldsymbol{v}2}, \phi_{\boldsymbol{v}1}) \in \mathbb{L}^2_x \times \mathbb{L}^2_y \end{cases} \tag{4.20}$$

Unlike for the configuration A, we are not able here to give an explicit resolution to the bending limit problem. We shall use finite element method to give an approximate solution. Of course, there is no membrane locking since we discretize the space of inextensional displacements.

Let $\mathbb{G}_n$ a set of spaces discretizing the space $\mathbb{L}^2_x \times \mathbb{L}^2_y$, i.e.

$$\begin{gathered} \forall (\phi_{\boldsymbol{v}2}, \phi_{\boldsymbol{v}1}) \in \mathbb{L}^2_x \times \mathbb{L}^2_y, \exists (\phi_{\boldsymbol{v}_n 2}, \phi_{\boldsymbol{v}_n 1}) \in \mathbb{V}_n \text{ such that} \\ (\phi_{\boldsymbol{v}_n 2}, \phi_{\boldsymbol{v}_n 1}) \xrightarrow{n \to \infty} (\phi_{\boldsymbol{v}2}, \phi_{\boldsymbol{v}1}). \end{gathered}$$

Then the Galerkin approximation onto $\mathbb{G}_n$ of the alternate formulation of the bending limit problem is :

$$\begin{cases} \text{Find } (\phi_{\boldsymbol{u}_n 2}, \phi_{\boldsymbol{u}_n 1}) \in \mathbb{V}_n, \text{ such that } \forall (\phi_{\boldsymbol{v}_n 2}, \phi_{\boldsymbol{v}_n 1}) \in \mathbb{G}_n \\ \int_\Omega \begin{pmatrix} \phi_{\boldsymbol{u}_n 2} \\ \phi_{\boldsymbol{u}_n 1} \end{pmatrix} \mathbb{A} \begin{pmatrix} \phi_{\boldsymbol{v}_n 2} \\ \phi_{\boldsymbol{v}_n 1} \end{pmatrix} ads = \langle \boldsymbol{f}, R^{-1}(\phi_{\boldsymbol{v}_n 2}, \phi_{\boldsymbol{v}_n 1}) \rangle \end{cases} \tag{4.21}$$

Classically, let $g_i = (\phi_{i2}, \phi_{i1})$ be a basis of $\mathbb{G}_n$ and let λ_i be the components of $(\phi_{\boldsymbol{u}_n 2}, \phi_{\boldsymbol{u}_n 1})$, solution of the alternate bending limit problem, in this basis :

$$(\phi_{\boldsymbol{u}_n 2}, \phi_{\boldsymbol{u}_n 1}) = \sum_i \lambda_i g_i \tag{4.22}$$

We are lead to solve the linear system of equation :

$$\sum_i a_{ij} \lambda_i = f_j \text{ for all j} \tag{4.23}$$

where the coefficients a_{ij} and f_j are given by

$$a_{ij} = \int_\Omega \begin{pmatrix} \phi_{i2} \\ \phi_{i1} \end{pmatrix} \mathbb{A} \begin{pmatrix} \phi_{j2} \\ \phi_{j1} \end{pmatrix} a\sqrt{a} dxdy \tag{4.24}$$

$$f_j = \int_\Omega \boldsymbol{f}.R^{-1}(\phi_{j2}, \phi_{j1}) a\sqrt{a} dxdy. \tag{4.25}$$

where the expression of the inextensional displacement $R^{-1}(\phi_{j2}, \phi_{j1})$ is given by the proposition 4.1:

$$\begin{aligned} R^{-1}(\phi_{j2}, \phi_{j1}) = & [cy\Phi_{j2}(x) - c\Psi_{j1}(y)]\, \boldsymbol{e}_1 \\ & + [c\Psi_{j2}(x) - cx\Phi_{j1}(y)]\, \boldsymbol{e}_2 - [\Phi_{j2}(x) - \Phi_{j1}(y)]\, \boldsymbol{e}_3, \end{aligned}$$

with

$$\Phi_{j\alpha}(z) = \int_0^z \phi_{j\alpha}(t)(z-t)dt, \qquad \Psi_{j\alpha}(z) = \int_0^z \phi_{j\alpha}(t)z(z-t)dt.$$

Remark 3. Except for the last expression of $R^{-1}(\phi_{j2}, \phi_{j1})$, this discretization of the bending limit problem holds for any hyperbolic shell. The principal difficulty would state in the computation of the coefficients of the right hand side f_j for which one have to solve a Goursat problem for the derived bending system (which is hyperbolic for hyperbolic shells). In the case of a hyperbolic paraboloid, this problem is trivially solved as in proposition 4.1, giving last expressions. On another hand the coefficient a_{ij} of (4.24) are easily computed by simple numerical integration.

Thus, choosing the set of discrete spaces $\mathbb{V}_n$, we are able to construct the solution of the bending limit problem. For simplicity, We have chosen continuous P_1 elements on each interval $[0,1]$. We define a basis $g_i = (\phi_{i2}, \phi_{i1})$ of $\mathbb{V}_n$ such that

$$\begin{aligned} g_i &= (\phi_{i2}, 0) && for \quad 1 \le i \le n \\ g_i &= (0, \phi_{i1}) && for \quad n+1 \le i \le 2n. \end{aligned}$$

The solution in displacement is then given by :

$$\begin{aligned} \boldsymbol{u}(x,y) = \sum_j x_j \big[&\left[cy\Phi_{j2}(x) - c\Psi_{j1}(y) \right] \boldsymbol{e}_1 \\ &+ \left[c\Psi_{j2}(x) - cx\Phi_{j1}(y) \right] \boldsymbol{e}_2 - \left[\Phi_{j2}(x) - \Phi_{j1}(y) \right] \boldsymbol{e}_3 \big]. \end{aligned} \tag{4.26}$$

To make the computation of the coefficient a_{ij}, we wrote a code which consists in 12 nodes numerical integration on each triangle of diameter $1/n$. It should be noticed that no effort have been done for optimizing of the procedure. We made the computation for several values of n, until $n = 64$, and solved the linear system (4.23) with usual Gauss method. We chose as limit value the results given with $n = 64$ since we constated the convergence.

As in the preceding example, with $E = 28500$, $\nu = 0.3$, we display some results obtained for the normal component of the displacement at point E=(0.5,0.5), taking various values of c, see table 2.

$c = 0.1$	$c = 0.5$	$c = 1$	$c = 2$	$c = 3$	$c = 5$
1.0284e-05	1.1103e-05	1.3428e-05	2.3835e-05	4.3350e-05	1.1789e-04

Table 2: Values of the normal component $u_3(E)$ for various geometries

4.4 Remark on the regularity of the solution of the bending limit problem

Classically, the inextensional displacement is smoother than general displacement in $\boldsymbol{V}$. As they satisfy the bending system 3.1, one can show that the tangential components $u_\alpha \in \boldsymbol{H}^2(\Omega)$, and the normal components $u_3 \in H^3(\Omega)$, [14, 10].

Since the bending limit problem (2.2) stands in the Lax-Milgram framework, For smooth external applied forces, one may expect additional regularity for the solution. But it is not true as the constrained problem (in subspace $R(S)$) is not elliptic. In fact the constraint implies a Lagrange multiplier that modifies the structure of the partial differential

equations[5, 21]. As we shall show, with an example the limit problem(2.2) does not enjoy local regularity properties which are classical for elliptic problems. We give here an example where the external force is in C^∞, but the solution of (3.8) is not in C^2.

It is based on the configuration A of section 4.2, the totally non-inhibited hyperbolic paraboloid clamped along a generator. Consider now, a slightly different configuration, we shall refer as configuration $\tilde{A}$, of hyperbolic paraboloid such that the non-inhibited of configuration $\tilde{A}$ part is exactly the same as configuration A. If the external forces are the same, say uniform and normal to the surface ($\boldsymbol{f} = f\boldsymbol{a}_3$), then the corresponding bending limit problems will be identical, giving the same solution. As an example of configuration $\tilde{A}$ we can take a larger rectangle

$$\tilde{\Omega} = [x_{00}, x_1] \times [y_0, y_1],$$

clamped along the boundary

$$\Gamma = \{x = x_{00}, \quad y \in [y_0, y_1]\} \cup \{y = y_0, \quad x \in [x_{00}, x_0]\} \cup \{y = y_1, \quad x \in [x_{00}, x_0]\}.$$

The surface (hyperbolic paraboloid) is still defined with

$$\boldsymbol{r}(x, y) = x\boldsymbol{e}_1 + y\boldsymbol{e}_2 + cxy\boldsymbol{e}_3,$$

In this case, although the external forces are C^∞, we show that the normal component of

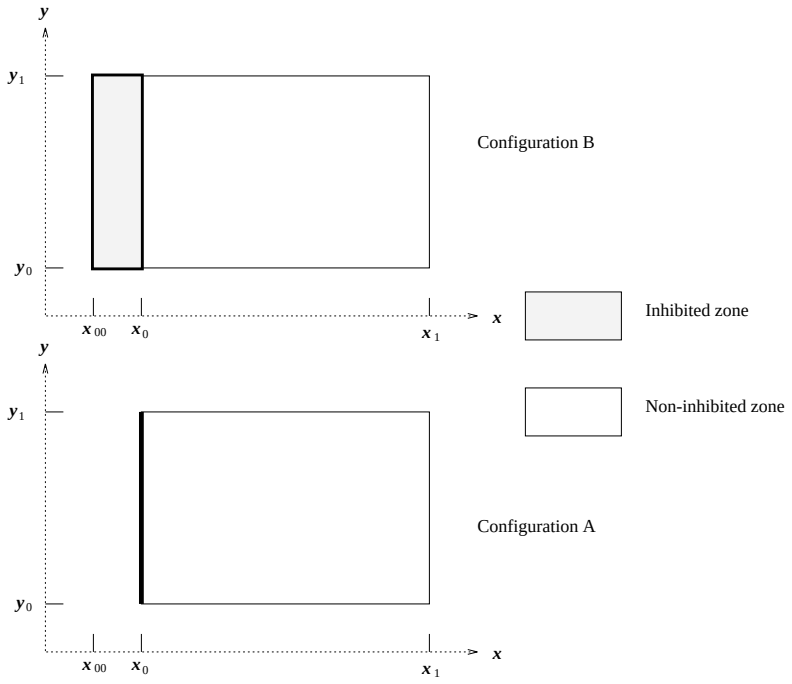

Figure 3: Configurations A and $\tilde{A}$ with same non-inhibited zone

the solution $\boldsymbol{u}^0$ of the corresponding bending limit problem is in $C^1(\tilde{\Omega})$ but not in $C^2(\tilde{\Omega})$.

Taking, the solution $\boldsymbol{u}^0$ given in proposition 4.2, we have

$$u_3(x, y) = \frac{-(cycy + 1)\Phi_{\boldsymbol{u}2}(x) - c^2 x \Psi_{\boldsymbol{u}2}(x)}{\sqrt{a(x, y)}}$$

We have

$$\Phi_{\boldsymbol{u}2}^{\prime\prime(x)} = \phi_{\boldsymbol{u}2}(x)$$

And, according to proposition 4.2, with $E = 28500$, $\nu = 0.3$, $x_0 = -1$, $x_1 = 1$, $y_0 = -1$, $y_0 = 1$, $f = -1$ and $c = 3$, we have

$$\phi_{\boldsymbol{u}2}(x_0) = 2.7219e - 05 \neq 0.$$

This obviously indicates that the second order partial derivatives in direction x of the normal component u_3 is different from zero on $x = x_0^+$, whereas for $x \in [x_{00}, x_0[$, the solution $\boldsymbol{u}^0$ is zero. This shows a discontinuity of the second order partial derivative of the normal component along the curve at $x = x_0$.

5 Numerical tests for the membrane locking on computation of non-inhibited hyperbolic shells

In this section, we present some numerical results concerning the Koiter's problem (2.1) with applied external forces (2.3) by classical finite element and we compare them with the solution of the corresponding bending limit problem (2.2) of configuration A and $\tilde{A}$ of section 4.

Our purpose here is to present validated computations of non-inhibited hyperbolic shells. For that we chose a finite-element and a mesh topology, we believe to be more robust with respect to membrane locking in the case considered.This doesn't mean that the chosen element is membrane locking free or is the best element for computation of thin elastic shells.

On another hand, it can be more interesting to consider other widely used schemes, such as DKT or 3-D general shell elements and chose various mesh topology and show how and when the membrane locking appears awkward in the computations.This can be done separatly using the validated computations we present here for comparison.

We shall use the Ganev-Argyris'scheme implemented on the INRIA's MODULEF code. The computations were performed on SUN's Solaris Ultra-SPARC. We used numerical integration with 12 nodes, exact for polynomial of order 6.

The Ganev-Argyris'scheme is a conforming scheme of high order polynomials which uses the $\mathbb{P}_4$-Ganev triangle for the approximation of the tangent components of the displacement, and the $\mathbb{P}_5$-Argyris triangle for the normal component; there are $15+15+21=51$ degrees of freedom in each triangle. The order of convergence is $O(h^4)$, where h is the diameter of the triangulation, preserved with the reduced integration scheme exact for polynomial of order 6. We refer to [3] for a complete description of the method.

Following the diagram (2.4) we shall consider various values of the thickness ϵ with various values of the mesh step h.

Diameter h	1/3	1/5	1/7	1/9	1/11	1/13	1/15	1/17
Nodes	85	221	421	685	1013	1405	1625	2281
DoF	600	1532	2896	4692	6920	9580	12672	16196

Table 3: Correspondence between the Diameter of the triangulation, the number of nodes and the number of Degrees of Freedom for Ganev-Argyris

The meshes chosen for our study follow the topological disposition of figure 4 and figure 5, respectively for the case of totally non-inhibited hyperbolic paraboloid (Configuration A) and the case of partially non-inhibited hyperbolic paraboloid (Configuration B). It should be noticed that in both cases the triangles follow the asymptotic lines (i.e the generators) of the hyperbolic paraboloid. Up to our knowledge, the chosen mesh topology is optimal, in our cases, to alleviate the locking phenomenon.

Of course, if one wants to test the locking robustness of a shell procedure using the benchmark bellow, such mesh optimization, taking in account particular geometric property, should be avoided. Actually, we have made computations on different mesh topologies with Ganev-Argyris element. We found that the locking appeared for much bigger thickness and acceptable approximations demand much more refinement of the mesh.

For each configuration we display the value of the normal component of the displacement at a point, for different values of the mesh step and of the thickness. We then plot the results in two different ways, following the diagram (2.4) : with fixed thickness ϵ and $h \to 0$

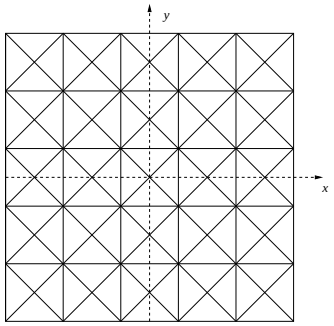

Figure 4: Mesh topology for configuration A ($h = 1/5$).

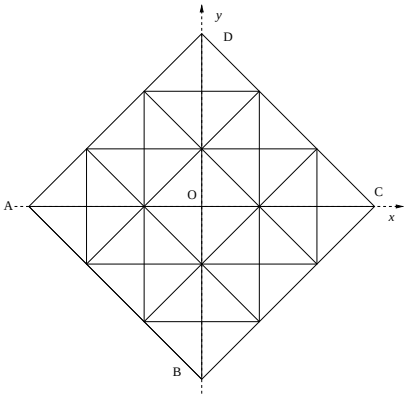

Figure 5: Mesh topology for the configuration B ($h = 1/3$).

to illustrate the convergence of the results then with fixed mesh step h and thickness $\epsilon \to 0$ to detect the locking.

In both cases, we see that for fixed thickness ϵ and $h \to 0$, the results seems to converge to a limit, which is coherent with the convergence theorem for the Ganev-Argyris scheme (figures 6 and 8). By the same time the result for fixed mesh h step and thickness $\epsilon \to 0$ shows the locking phenomenon(figures 7 and 9).

5.1 Configuration A – Case of the totally non-inhibited hyperbolic paraboloid

We recall that the shell is clamped along a generator and admits inextensional displacement everywhere, see proposition 4.2. As in subsection 4.2, we take $c = 3$, $E = 28500$, $\nu = 0.3$, $x_0 = -1$, $x_1 = 1$, $y_0 = -1$ and $y_0 = 1$ and $\boldsymbol{f}^\epsilon = \epsilon^3 \boldsymbol{a}_3$. We display the values of the normal component at point (1,1) in table 4 and we plot them in figure 6 and figure 7. In this case the value at (1,1) of the normal component of the solution $\boldsymbol{u}^0$ of the bending limit problem is

$$u_3^0 = 1.4429 \times 10^{-03}$$

$h\backslash\epsilon$	1.10^{-2}	5.10^{-3}	2.10^{-3}	1.10^{-3}	5.10^{-4}	2.10^{-4}	1.10^{-5}	5.10^{-5}	2.10^{-5}	1.10^{-5}
1/2	1.2041	1.0311	0.7064	0.3948	0.1571	0.0421	0.0222	0.0163	0.0109	0.0055
1/3	1.2352	1.0068	0.6992	0.5275	0.4034	0.2676	0.1678	0.0738	0.0171	0.0064
1/4	1.5293	1.4921	1.4490	1.4006	1.3198	1.0846	0.7908	0.4755	0.2156	0.1249
1/5	1.5152	1.4994	1.3667	1.2935	1.2181	1.0528	0.8705	0.6665	0.4044	0.2195
1/6	1.5357	1.5107	1.4895	1.4762	1.4630	1.4311	1.3603	1.1912	0.8164	0.5581
1/7	1.5342	1.5057	1.4749	1.4521	1.4321	1.4044	1.3569	1.2530	1.0340	0.8166
1/8	1.5357	1.5109	1.4907	1.4793	1.4696	1.4592	1.4501	1.4305	1.3537	1.1796
1/9	1.5354	1.5103	1.4892	1.4765	1.4656	1.4541	1.4450	1.4264	1.3553	1.2445
1/10	1.5355	1.5108	1.4913	1.4806	1.4719	1.4627	1.4575	1.4516	1.4419	1.4095
1/11	1.5355	1.5108	1.4912	1.4805	1.4718	1.4627	1.4570	1.4512	1.4291	1.3741
1/12	1.5354	1.5108	1.4915	1.4812	1.4730	1.4644	1.4591	1.4545	1.4501	1.4377
1/13	1.5353	1.5108	1.4915	1.4813	1.4732	1.4647	1.4596	1.4547	1.4492	1.4374

Table 4: Configuration A – Normal component $u_3 \times 10^{-03}$ at point (1,1)

From figure 6 one can see the convergence of the displacement for fixed thickness as the mesh step $h \to 0$. We conclude that the results obtaixned by Ganev-Argyris are accurate, for the finest mesh, even when $\epsilon = 10^{-5}$.

It is interesting to notice that the convergence (when the thickness $\epsilon \to 0$ towards the solution of the bending limit problem is very quick : even for $\epsilon = 10^{-2}$ the difference with the limit solution is only 6%.

Looking at figure 7, except for the finest meshes $h = 1/13$ and $h = 1/11$, one can see the locking effect as the thickness $\to 0$. In fact, for the mesh $h = 1/13$, the locking is present but apppears awkward only for smaller thicknesses than $\epsilon = 10^{-05}$.

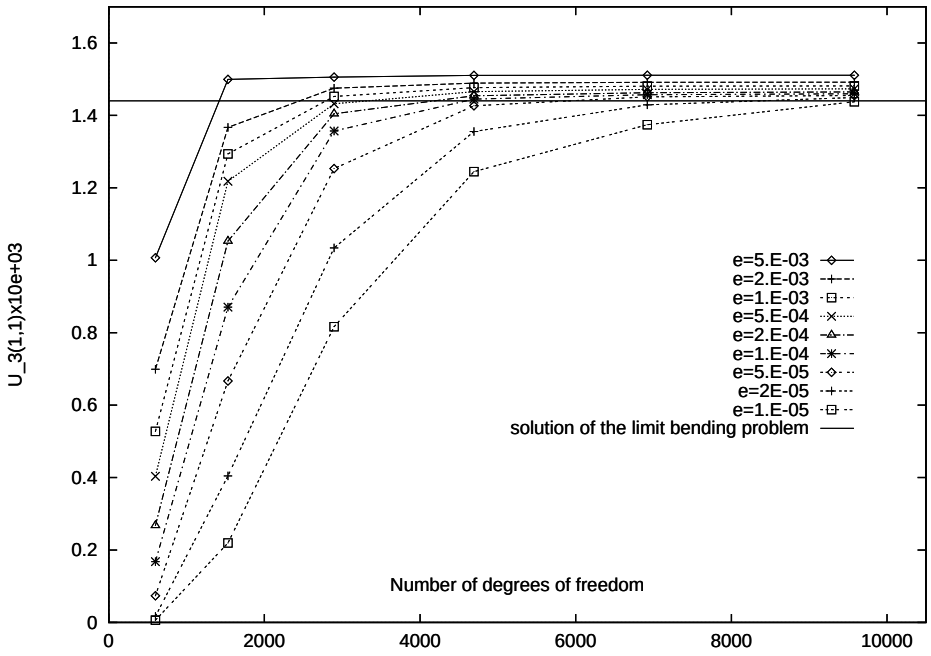

Figure 6: Configuration A – Plotting of $u_3(1,1) \times 10^3$ at constant thickness and $h \to 0$

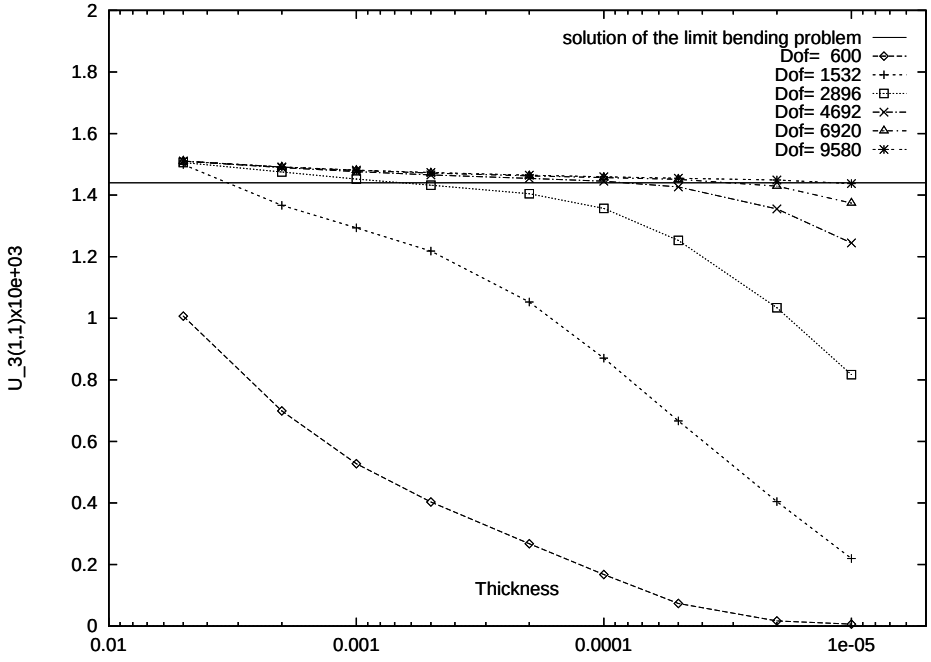

Figure 7: Configuration A – Plotting of $u_3(1,1) \times 10^3$ at constant mesh step and thickness $\epsilon \to 0$

5.2 Configuration B – Case of the partially non-inhibited hyperbolic paraboloid

We consider here the configuration B described in subsection 4.3. It is the hyperbolic paraboloid defined by the four points

$$\begin{array}{ll} A:(-1,0) & B:(0,-1) \\ C:(1,0) & D:(0,1) \end{array}$$

The paraboloid is clamped along the border AB. The shell is non-inhibited, but has a inhibited part $A)B$, see the proposition 4.3 and the figure 2.

We take $c = 3$, $E = 28500$, $\nu = 0.3$ and $\boldsymbol{f}^\epsilon = \epsilon^3 \boldsymbol{a}_3$.

Remark 4. This example is very similar to the one studied in [12] and [6], recommended as a test for shell procedures in [7].

We display the values taken by the normal component at point $(0.5, 0.5)$, in table 5 and we plot them in figure 8 and figure 9. In this case the value at (0.5,0.5) of the normal component of the solution $\boldsymbol{u}^0$ of the bending limit problem is

$$u_3^0(0.5, 0.5) = 4.3350 \times 10^{-05}$$

$h\backslash\epsilon$	1.10^{-2}	5.10^{-3}	2.10^{-3}	1.10^{-3}	5.10^{-4}	2.10^{-4}	1.10^{-5}	5.10^{-5}	2.10^{-5}	1.10^{-5}
1/2	5.7083	4.3985	2.2945	1.1446	0.6200	0.4278	0.3710	0.2885	0.1550	0.0366
1/3	5.4458	4.8254	3.6582	2.5921	1.7495	1.2362	1.1140	1.0409	0.8232	0.4841
1/4	6.3178	5.8110	5.0627	4.1816	3.2264	2.3942	2.1474	2.O504	1.8827	1.5013
1/5	6.0824	5.6280	5.1274	4.6036	3.8821	3.0221	2.6767	2.5426	2.4675	2.3519
1/6	6.4090	5.9298	5.4748	5.1088	4.5756	3.7380	3.2987	3.0928	3.0087	2.9680
1/7	6.2903	5.8184	5.3862	5.1030	4.7375	4.0467	3.5836	3.3199	3.2031	3.1773
1/8	6.4661	5.9776	5.5343	5.2736	4.9927	4.4308	3.9624	3.6434	3.4779	3.4457
1/9	6.3964	5.9118	5.4705	5.2216	4.9915	4.5590	4.1325	3.7889	3.5778	3.5334
1/10	6.5061	6.0117	5.5602	5.3094	5.0968	4.7514	4.3723	4.0143	3.7554	3.6938
1/11	6.4597	5.9685	5.5179	5.2682	5.0687	4.7853	4.4667	4.1197	3.8263	3.7463
1/12	6.5346	6.0370	5.5795	5.3259	5.1281	4.8804	4.6121	4.2830	3.9600	3.8584
1/13	6.5014	6.0064	5.5498	5.2962	5.1004	4.8769	4.6542	4.3564	4.0196	3.8983
1/14	6.5555	6.0562	5.5950	5.3382	5.1407	4.9287	4.7386	4.4719	4.1277	3.9857
1/15	6.5305	6.0334	5.5731	5.3163	5.1189	4.9149	4.8000	4.5176	4.1795	4.0199
1/16	6.5714	6.0712	5.6075	5.3484	5.1491	4.9477	4.7979	4.5959	4.2678	4.0933
1/17	6.5518	6.0535	5.5907	5.3316	5.1321	4.9331	4.7979	4.6201	4.3108	4.1257

Table 5: Configuration B – Normal component $\times 10^{-05}$ at point (0.5,0.5)

From figure 8 point of view, one can see the for each thickness ϵ fixed, the values of $u_3(0.5, 0.5)$ converge to a limit, we can extrapolate. We then see that these extrapolated limit converge to the value given by the solution of the bending limit problem. This validate the results obtained for the finest mesh ($h = 1/17$), at least for thickness $\epsilon > 10^4$. For smaller thickness, the shift of convergence due to locking is too important, see figure 9.

We also note that the convergence towards the solution of the bending limit problem is not as fast as in the preceding case with rectangular shape. This is due to the fact that the limit solutions don't take in account the inhibited zone. Two different problems in this

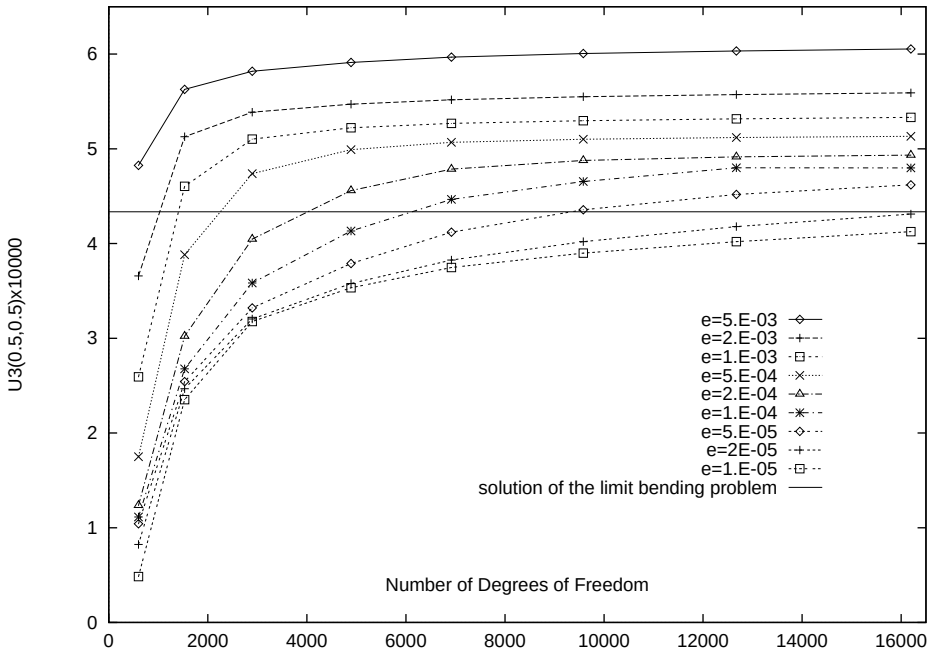

Figure 8: Configuration B – Plotting of $u_3(E) \times 10^5$ at constant thickness $h \to 0$

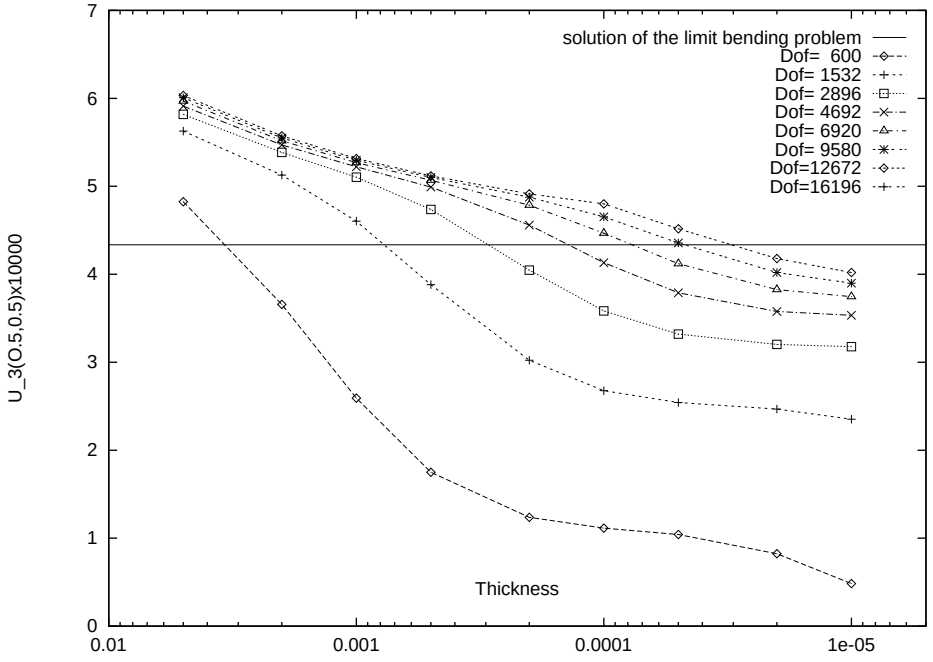

Figure 9: Configuration B – Plotting of $u_3(E) \times 10^5$ at constant mesh step and thickness $\epsilon \to 0$

configuration, with same external forces and boundary conditions on identical non-inhibited zone, give the same bending limit solution as in subsection 4.4.

Remark 5. In [12] some computation were made on a similar case of non-inhibited hyperbolic shell with reduced numerical integration. It was asserted that low precision schemes eliminate the locking in the sense where the results don't converge to zero, but give wrong approximation in comparison with converging higher precision schemes. The validation here, comfort the assertion that reduced numerical integration is not a remedy to the locking.

References

[1] J.-L. Akian and E. Sanchez-Palencia, *Approximation de coques élastiques minces par facettes planes. phénomènes de blocage membranaire*, C. R. Acad. Sci. Série I, 315 (1992), pp. 363–369.

[2] I. Babuska and M. Suri, *On locking and robustness in the finite element methods*, SIAM Journal of Numerical Analysis, 29 (1992), pp. 261–293.

[3] M. Bernadou, *Méthodes d'éléments finis pour les problèmes de coques minces*, Masson, Paris, 1994.

[4] M. Bernadou and P. G. Ciarlet, *Sur l'ellipticité du modèle linéaire des coques de w. t. koiter*, in Computing Methods in Sciences and Engineering, Lectures notes in Economics and Math. Systems, Springer, 1976, pp. 89–136.

[5] F. Brezzi, P. Gérard, and E. Sanhez-Palencia, *Remarks on ellipticity and regularity for shells and other constrained systems*, C. R. Acad. Sci. Série I, 326 (1998), pp. 1155–1162.

[6] D. Chapelle, *Etude de phénomène de verrouillages numérique pour les problèmes de coques minces*, PhD thesis, Université Pierre et Marie Curie (Paris VI), 1996. Laboratoire des Ponts et Chaussées.

[7] D. Chapelle and K. J. Bathe, *Fundamental considerations for the finite element analysis of shell structures*, Computers and Structures, 66 (1998), pp. 19–36.

[8] D. Chenais and J.-C. Paumier, *On the locking phenomenon for a class of elliptic problems*, Numerische Mathematik, 67 (1994), pp. 427–440.

[9] D. Choï, *Rigidité infinitésimale d'un type de pli d'une surface en déplacement inextensionnel*, C. R. Acad. Sci Série I, 317 (1993), pp. 323–327.

[10] ——, *On geometrical rigidity of surfaces. application to the theory of thin elastic shells*, Mathematical Models and Methods in Applied Science, 7(4) (1997), pp. 507–555.

[11] ——, *Résolution du problème limite des coques élastiques en flexion dans le cas d'un paraboloïde hyperbolique*, C. R. Acad. Sci Série II b, 324 (1998), pp. 427–434.

[12] D. Choï, F. J. Palma, E. Sanchez-Palencia, and M. A. Vilariño, *Remarks on membrane locking in the finite element computation of very thin elastic shells*, Modélisation Mathématique et Analyse Numérique, 32 (1998), pp. 131–152.

[13] G. Darboux, *Théorie générale des surfaces*, vol. 4, Gauthier-Villars, 1896.

[14] G. Geymonat and E. Sanchez-Palencia, *On rigidity of certain surfaces with edges and application to shell theory*, Arch. Rat. Mech. Anal., 129 (1995), pp. 11–45.

[15] J.-L. Lions and E. Sanchez-Palencia, *Problèmes aux limites sensitifs*, C. R. Acad. Sci. série I, 319 (1995), pp. 1021–1026.

[16] J. Pitkaranta, *The problem of membrane locking in finite elements analysis of cylindrical shells*, Numerische Mathematik, 61 (1992), pp. 523–542.

[17] J. Sanchez-Hubert and E. Sanchez-Palencia, *Coques élastiques minces : Propriétés asymptotiques*, Masson, 1997.

[18] E. SANCHEZ-PALENCIA, *Statique et dynamique des coques minces, I et II*, C. R. Acad. Sci. Paris série I, (1989), pp. 411–417 et 531–537.

[19] ——, *Passage à la limite de l'élasticité tridimensionnelle à la théorie asymptotique des coques minces.*, Compt. Rend. Acad. Sci. Paris, 311, série II, p. 909-916, (1990).

[20] ——, *Asymptotic and spectral properties of a class of singular-stiff problems*, Journal des Mathématiques Pures et Appliquées, 71 (1992), pp. 379–406.

[21] ——, *On sensitivity and related phenomena in thin shells which are not geometrically rigid*, Mathematical Models and Methods in Applied Science, (1998).

[22] M. SPIVAK, *A comprehensive introduction to differential geometry*, vol. 5, Publish or Perish Inc., 1975.

[23] I. N. VEKUA, *Generalized analytic functions*, Pergamon Press, 1959. English translation.